REPORT DOCUMENTATION PAGE	Form Approved OMB No. 0704-0188

1. REPORT DATE (DD-MM-YYYY)	2. REPORT TYPE	3. DATES COVERED (From - To)
02-08-2011	Journal Article	

4. TITLE AND SUBTITLE

Fertilization Potential of Volcanic Dust in the Low-nutrient Low-chlorophyll Western North Pacific Subtropical Gyre: Satellite Evidence and Laboratory Study

5a. CONTRACT NUMBER	
5b. GRANT NUMBER	
5c. PROGRAM ELEMENT NUMBER	N/A

6. AUTHOR(S)

I.-I. Lin, Chuanmin Hu, Yuan-Hui Li, Tung-Yuan Ho, Tobias P. Fischer, George T.F. Wong, Jingfeng Wu, Chih-Wei Huang, D. Allen Chu, Dong S. Ko and Jen-Ping Chen

5d. PROJECT NUMBER	NNS04AA801
5e. TASK NUMBER	
5f. WORK UNIT NUMBER	73-8669-A8-5

7. PERFORMING ORGANIZATION NAME(S) AND ADDRESS(ES)

Naval Research Laboratory
Oceanography Division
Stennis Space Center, MS 39529-5004

8. PERFORMING ORGANIZATION REPORT NUMBER

NRL/JA/7320--09-9113

9. SPONSORING/MONITORING AGENCY NAME(S) AND ADDRESS(ES)

NASA Headquarters
Attn: Laurie Friederich
Mail Code 210.H, Bldg. 17, Rm. N111
Greenbelt, MD

10. SPONSOR/MONITOR'S ACRONYM(S)

NASA

11. SPONSOR/MONITOR'S REPORT NUMBER(S)

12. DISTRIBUTION/AVAILABILITY STATEMENT

Approved for public release, distribution is unlimited.

13. SUPPLEMENTARY NOTES

14. ABSTRACT

In the western North Pacific subtropical ocean, the Anatahan volcano of the Mariana Islands erupted on 10 May 2003 for the first time in recorded history. Based on nine different types of remote sensing data provided by NASA, laboratory experiment of the Anatahan samples, and a 3-D ocean circulation model developed by the U.S. Naval Research Laboratory, the post volcanic ocean biogeochemical response to the Anatahan eruption was explored. It was observed that soon after the eruption, the aerosol optical depth abruptly increased from the pre-eruption loading of ~0.1 to ~2. In the week following the eruption, a "bloom-like" patch was observed by NASA's Aqua Moderate Resolution Imaging Spectroradiometer (MODIS) ocean color sensor. Based on the chlorophyll a, fluorescence line height (FLH), at-sensor total radiance, and normalized water-leaving radiance data obtained by MODIS, the cause of the bloom-like patch was diagnosed. The results suggest that the patch was most likely a mixture of suspended volcanic particles and a phytoplankton bloom. FLH was found to be ~9 -17 × 10^{-3} mW cm^{-2} μm^{-1} sr^{-1} in the patch and ~3 -5 × 10^{-3} mW cm^{-2} μm^{-1} sr^{-1} in the ambient water, indicating that a 2 -5-fold increase in biological activity occurred during the week following the eruption. Satellite altimetry indicated that the bloom took place in the presence of downwelling and was not a result of upwelled nutrients in this oligotrophic ocean. Analysis of satellite ocean color spectra of the bloom region found similar spectra as the reference Trichodesmium spectra. Laboratory experiments further substantiate the satellite observations which show elevated concentrations of limiting nutrients provided by the Anatahan samples.

15. SUBJECT TERMS

Fertilization potential of volcanic dust, ocean biogeochemical response, ocean color, MODIS, EASNFS.

16. SECURITY CLASSIFICATION OF:			17. LIMITATION OF ABSTRACT	18. NUMBER OF PAGES	19a. NAME OF RESPONSIBLE PERSON
a. REPORT	b. ABSTRACT	c. THIS PAGE			Dong S. Ko
Unclassified	Unclassified	Unclassified	UL	12	19b. TELEPHONE NUMBER (Include area code) (228) 688-5448

Fertilization potential of volcanic dust in the low-nutrient low-chlorophyll western North Pacific subtropical gyre: Satellite evidence and laboratory study

I.-I. Lin,[1] Chuanmin Hu,[2] Yuan-Hui Li,[3] Tung-Yuan Ho,[4] Tobias P. Fischer,[5] George T. F. Wong,[4,6] Jingfeng Wu,[7] Chih-Wei Huang,[1,4] D. Allen Chu,[8] Dong S. Ko,[9] and Jen-Ping Chen[1]

Received 14 December 2009; revised 15 August 2010; accepted 24 September 2010; published 26 February 2011.

[1] In the western North Pacific subtropical ocean, the Anatahan volcano of the Mariana Islands erupted on 10 May 2003 for the first time in recorded history. Based on nine different types of remote sensing data provided by NASA, laboratory experiment of the Anatahan samples, and a 3-D ocean circulation model developed by the U.S. Naval Research Laboratory, the postvolcanic ocean biogeochemical response to the Anatahan eruption was explored. It was observed that soon after the eruption, the aerosol optical depth abruptly increased from the pre-eruption loading of ~0.1 to ~2. In the week following the eruption, a "bloom-like" patch was observed by NASA's Aqua Moderate Resolution Imaging Spectroradiometer (MODIS) ocean color sensor. Based on the chlorophyll *a*, fluorescence line height (FLH), at-sensor total radiance, and normalized water-leaving radiance data obtained by MODIS, the cause of the bloom-like patch was diagnosed. The results suggest that the patch was most likely a mixture of suspended volcanic particles and a phytoplankton bloom. FLH was found to be ~9–17 × 10^{-3} mW cm^{-2} μm^{-1} sr^{-1} in the patch and ~3–5 × 10^{-3} mW cm^{-2} μm^{-1} sr^{-1} in the ambient water, indicating that a 2–5-fold increase in biological activity occurred during the week following the eruption. Satellite altimetry indicated that the bloom took place in the presence of downwelling and was not a result of upwelled nutrients in this oligotrophic ocean. Analysis of satellite ocean color spectra of the bloom region found similar spectra as the reference *Trichodesmium* spectra. Laboratory experiments further substantiate the satellite observations which show elevated concentrations of limiting nutrients provided by the Anatahan samples, and the averaged soluble nitrate, phosphate, and Fe were 42, 3.1, and 2.0 nM, respectively. Though it was not possible to obtain in situ observations of the ocean biogeochemical responses that followed the Anatahan eruption, this study provided evidence based on remote sensing data and laboratory experiment that fertilization of volcanic aerosols occurred following this eruption in one of the most oligotrophic low-nutrient low-chlorophyll ocean deserts on Earth.

Citation: Lin, I.-I., et al. (2011), Fertilization potential of volcanic dust in the low-nutrient low-chlorophyll western North Pacific subtropical gyre: Satellite evidence and laboratory study, *Global Biogeochem. Cycles*, *25*, GB1006, doi:10.1029/2009GB003758.

[1]Department of Atmospheric Sciences, National Taiwan University, Taipei, Taiwan.
[2]College of Marine Sciences, University of South Florida, St. Petersburg, Florida, USA.
[3]Department of Oceanography, School of Ocean and Earth Science and Technology, University of Hawai'i at Mānoa, Honolulu, Hawaii, USA.
[4]Research Centre for Environmental Changes, Academia Sinica, Taipei, Taiwan.
[5]Department of Earth and Planetary Sciences, University of New Mexico, Albuquerque, New Mexico, USA.
[6]Institute of Hydrology and Ocean Sciences, National Central University, Jungli, Taiwan.
[7]Rosenstiel School of Marine and Atmospheric Science, University of Miami, Miami, Florida, USA.
[8]Goddard Earth Sciences and Technology Center, NASA Goddard Space Flight Center, Greenbelt, Maryland, USA.
[9]Naval Research Laboratory, Stennis Space Center, Mississippi, USA.

0886-6236/11/2009GB003758

1. Introduction

[2] Marine primary production is a key component in the global carbon cycle [*Canadell et al.*, 2007]. The open ocean, which accounts for about three quarters of the global marine primary production [*Pauly and Christensen*, 1995], is of course a significant contributor. Yet, there are still major unresolved issues in understanding the controlling mechanisms of primary production in these waters. For example, the conventional wisdom, which invokes wintertime convection and diapycnal diffusion for supplying nutrients to the euphotic zone to support photosynthetic activities, has been found to be insufficient for providing the nutrients needed for sustaining the observed primary production [*McGillicuddy and Robinson*, 1997]. As a result, a number of novel mechanisms have been proposed for providing the "missing" nutrients [*McGillicuddy et al.*, 1998; *Villareal et al.*, 1999; *Uz et al.*, 2001; *Chen et al.*, 2007; *Lin et al.*, 2003, 2010]. Atmospheric deposition is another possibility and it is especially intriguing [*Berner et al.*, 1983; *Martin and Gordon*, 1988; *Broecker and Henderson*, 1998; *Falkowski et al.*, 1998; *Fung et al.*, 2000; *Bay et al.*, 2004; *Uematsu et al.*, 2004; *Capone et al.*, 2005; *Jickells et al.*, 2005; *Deutsch et al.*, 2007; *Duggen et al.*, 2007, 2010; *Lin et al.*, 2007, 2009; *Langmann et al.*, 2010]. Unlike the other proposed mechanisms which emphasize the supply of the macronutrients combined nitrogen and phosphate to the euphotic zone, atmospheric deposition can provide not only these two macronutrients but also the micronutrient iron [*Wu et al.*, 2001; *Jickells et al.*, 2005; *Duarte et al.*, 2006], which can stimulate nitrate uptake in nitrate-replete water [*Timmermans et al.*, 1994, 2004] and nitrogen fixation in oligotrophic water [*Karl et al.*, 1997; *Wong et al.*, 2002; *Capone et al.*, 2005].

[3] For several decades, research on the supply of nutrients to the oceans by atmospheric deposition has focused on desert dust [*Mahowald et al.*, 1999; *Fung et al.*, 2000; *Wu et al.*, 2000; *Johnson et al.*, 2003]. Meanwhile, it has been suggested that volcanic dust is a much-neglected aerosol source which may also provide nutrients to stimulate ocean biogeochemical responses [*Uematsu et al.*, 2004; *Jickells et al.*, 2005; *Duggen et al.*, 2007, 2010; *Langmann et al.*, 2010]. Laboratory research has indicated that volcanic dust has rapid fertilization potential [*Duggen et al.*, 2007]. However, due to the episodic and irregular nature of volcanic eruptions and their locations of occurrence, which are frequently remote, it has been difficult to conduct timely in situ investigations of oceanic responses to volcanic eruptions. Research on volcanic fertilization is still in its infancy, and very little direct evidence has been presented [*Uematsu et al.*, 2004; *Jickells et al.*, 2005; *Duggen et al.*, 2007, 2010; *Langmann et al.*, 2010]. This is especially true in the low-nutrient low-chlorophyll (LNLC) waters, since most current results report on findings in the high-nutrient low-chlorophyll (HNLC) waters [*Duggen et al.*, 2007, 2010].

[4] In the evening of 10 May 2003, the Anatahan volcano (146°E, 16°N) in the Northern Mariana Islands (Figure 1a) erupted for the first time in recorded history [*Nakada et al.*, 2005; *Wade et al.*, 2005]. This volcano is located in the western North Pacific Subtropical Gyre (WNPSG), a well-known LNLC ocean desert [*Levitus et al.*, 1993; *Karl*, 1999] (Figure 1b). The eruption in 2003 was a relatively large eruption of Volcanic Explosivity Index 3 [*Newhall and Self*, 1982; *Simkin and Siebert*, 1994; *Trusdell et al.*, 2005]. Due to the unavailability of in situ ocean biogeochemical observations, here, data from satellite remote sensing and laboratory experiment are used to study the biological response of the nearby LNLC water following the eruption and the deposition of volcanic ash to the surface ocean.

[5] Because dust particles suspended in water may be falsely interpreted as phytoplankton by band ratio chlorophyll algorithms [*Claustre et al.*, 2002; *Gin et al.*, 2003; *Duggen et al.*, 2007], this study used at-sensor total radiance, normalized water-leaving radiance, Fluorescence Line Height, and ocean color spectrum data from the Moderate Resolution Imaging Spectroradiometer (MODIS) onboard the NASA/Aqua satellite to study the postvolcanic ocean response to the Anatahan eruption. Other types of satellite data used were (1) aerosol optical depth (AOD) and true color data from MODIS [*Kaufman et al.*, 2002]; (2) TOPEX/Poseidon and JASON-1 altimetry sea surface height anomaly (SSHA) data [*Fu et al.*, 1994]; (3) Tropical Rainfall Measuring Mission/Microwave Imager (TMI) sea surface temperature (SST) data [*Wentz et al.*, 2000]; and (4) QuikSCAT sea surface wind vectors [*Liu et al.*, 1998]. In addition, a 3-D ocean circulation model (the East Asian Seas Nowcast/Forecast System, EASNFS) from the U.S. Naval Research Lab [*Ko et al.*, 2003; *Chapman et al.*, 2004] was employed to supplement satellite observations to understand the physical condition of the ocean. Further, laboratory experiment was conducted using the Anatahan volcanic samples [*de Moor et al.*, 2005; *Trusdell et al.*, 2005; *Wade et al.*, 2005] to analyze the available nutrients for ocean fertilization from the Anatahan event.

2. Eruption of the Anatahan Volcano

[6] Anatahan volcano rises from depths of ~3000 km below sea level to an elevation of 788 m above sea level and is a large stratovolcano that has erupted basalts and dacites. No volcanic activity has been documented before the May 2003 event. *de Moor et al.* [2005] suggest that Anatahan contained an extensive hydrothermal system based on the presence of Ca and S-bearing minerals in the May 2003 erupted ash. The formation of sulfate absorbed onto the ash is likely the result of oxidation of magmatic SO_2 in the eruption cloud [*de Moor et al.*, 2010].

[7] The 2003 eruption cloud reached 5.5 km on 11 May (first day of the eruption) and decreased to about 2–3 km on 18 May. The total amount of ash deposited on the island during the eruption was 0.024 Gt (1 Gt = 10^{12} g) and the total calculated eruption volume is 45.4×10^6 m^3 but is a lower estimate as it does not take into account the amount deposited into the ocean [*Trusdell et al.*, 2005]. This categorizes the May 2003 eruption of Anatahan as Volcanic Explosivity Index (VEI) 3 [*Newhall and Self*, 1982]. VEI 3 eruptions are fairly common and have occurred on average about 1000 times in 1000 years over the Holocene time period [*Simkin and Siebert*, 1994]. Therefore, in terms of eruption size, the 2003 Anatahan eruption was not unusual.

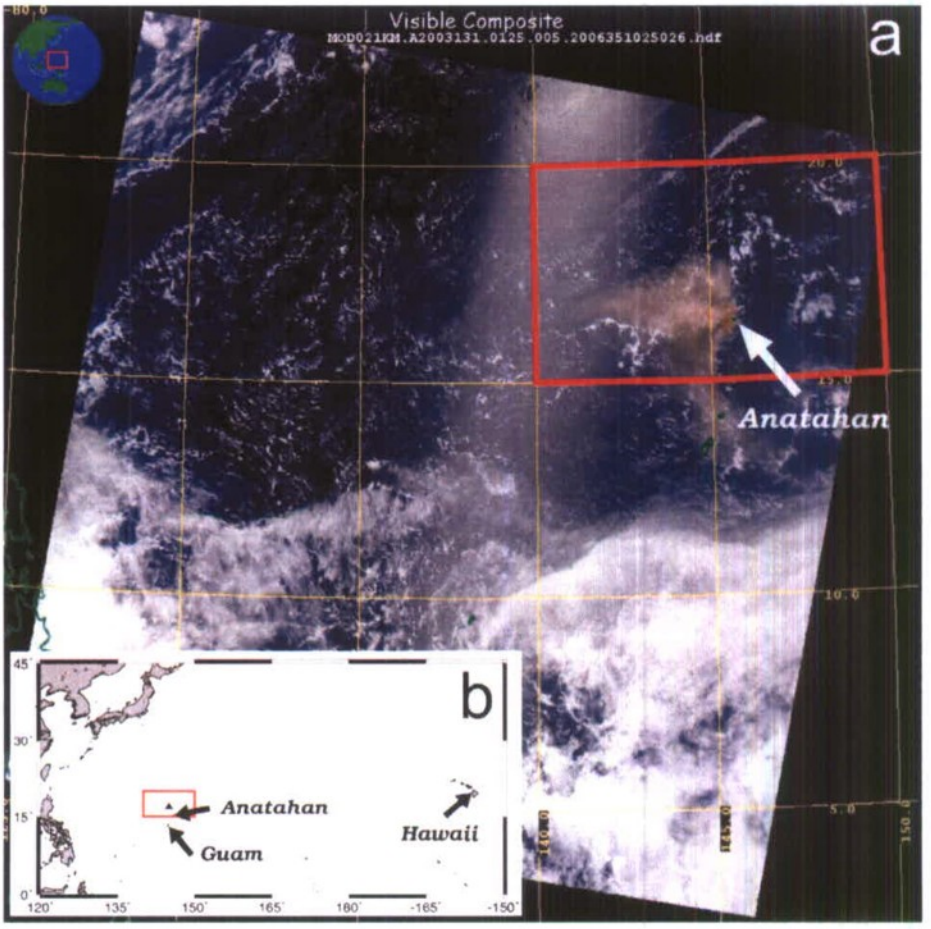

Figure 1. (a) MODIS true color image showing the volcanic plume (outlined by the red box; 140°E–150°E, 15°N–20°N) erupted from Anatahan on 11 May 2003. (b) Map showing the location of the red box in Figure 1a; the triangle depicts the location of the profile in Figure 8.

The high SO_2 emission which was in excess of what could have been dissolved in the erupted magma was identified by *de Moor et al.* [2005] and *Pallister et al.* [2005]. Eruptions that release "excess" sulfur [*Rose et al.*, 1982] are fairly common for silicic volcanoes located on subduction zones (see recent compilation in the work by *Wallace* [2005]). In the case of Anatahan, this excess sulfur was released into the atmosphere but approximately 25% of the erupted sulfur was adsorbed onto the ash (up to ~1700 mg S/kg ash) [*de Moor et al.*, 2005]. The proportion of adsorbed sulfur is similar to what has been documented for other eruptions where such measurements have been made, i.e., at Galunggung and Fuego volcanoes where approximately 35% of the emitted S was scavenged by ash [*de Hoog et al.*, 2001; *Rose*, 1977].

[8] As observed by the AOD data (daily, 1 degree spatial resolution level 3 data) from the MODIS atmospheric sensors onboard the NASA/Terra and Aqua satellites [*Kaufman et al.*, 2002], prior to the volcanic eruption, the WNPSG was characterized by the typical marine atmospheric condition of low aerosol loading with AOD < 0.1 (Figure 2a). Immediately after the eruption on 11 May 2003, MODIS-derived AOD abruptly increased to 1.0–2.0, nearly a twentyfold rise in aerosol loading at the downwind side of the island (Figure 2b). As also clearly depicted in the corresponding MODIS true color image, a large plume of volcanic dust spread westward from Mt. Anatahan approximately 500 km over the WNPSG (Figure 1a). A few days later (14–19 May), the AOD fell back to the pre-eruption level of around 0.1 (Figure 2c). Meanwhile, a U.S. National Science Foundation MARGINS team went to the Anatahan volcano to collect eruption samples for major and trace element analyses [*de Moor et al.*, 2005; *Trusdell et al.*, 2005; *Wade et al.*, 2005]. Laboratory analysis of the samples will be presented in section 6.

3. Exploration of the Postvolcanic Ocean Responses

[9] MODIS chlorophyll *a* (Chl *a*) image (level 2, 4 km spatial resolution data) obtained before the eruption depicted the typical WNPSG oligotrophic ocean condition with Chl *a* concentrations of about 0.05 mg m^{-3} (Figure 3a). Five days

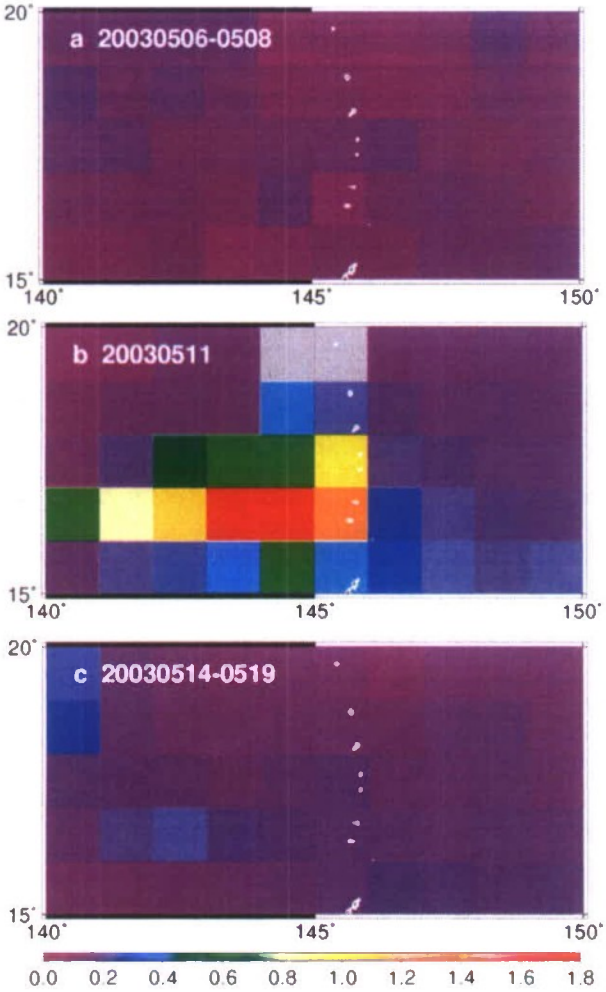

Figure 2. MODIS aerosol optical depth (AOD) images of the volcanic plume region (red box in Figure 1) (a) before, (b) during, and (c) after the volcanic eruption.

after the eruption on 15 May, the first-available cloud-free MODIS Chl *a* image showed a well-defined "bloom-like" patch in the area of 144°E–146.5°E and 16.5°N–17.5°N covering an area of about 7×10^3 km^2 (Figure 3b), which was the same location as the dust plume (Figures 1a and 2b). The next-available cloud-free MODIS Chl *a* image, which was obtained on 17 May 2003, revealed that the patch had elongated toward the northeast in the area between 145°E–147°E and 16.5°N–18.5°N (Figure 3c). However, this type of "standard" Chl *a* image alone is not sufficient to show that the bloom-like patch was indeed a phytoplankton bloom or an artifact due to the nonliving suspended volcanic particles in the water. This is because that MODIS Chl *a* concentration was estimated using a blue/green band ratio, but nonliving particles like suspended volcanic dust in the water can also cause a decrease in the blue/green ratio and therefore a false increase in the estimated Chl *a* concentration [*Claustre et al.*, 2002; *Duggen et al.*, 2007]. Therefore, additional ocean color information obtained using the at-sensor total radiance (L_t), normalized water-leaving radiance (nLw), and Fluorescence Line Height (FLH) was used in this study to aid diagnoses [*Hu et al.*, 2005; *Gilerson et al.*, 2007]. In addition, the bloom-like patch observed in this study was compared with the well-known phytoplankton bloom caused by equatorial upwelling.

[10] In Figures 3d and 3e, FLH images of the postvolcanic bloom-like patch observed on 15 and 17 May are shown (see the regions enclosed by boxes in Figures 3b and 3c for

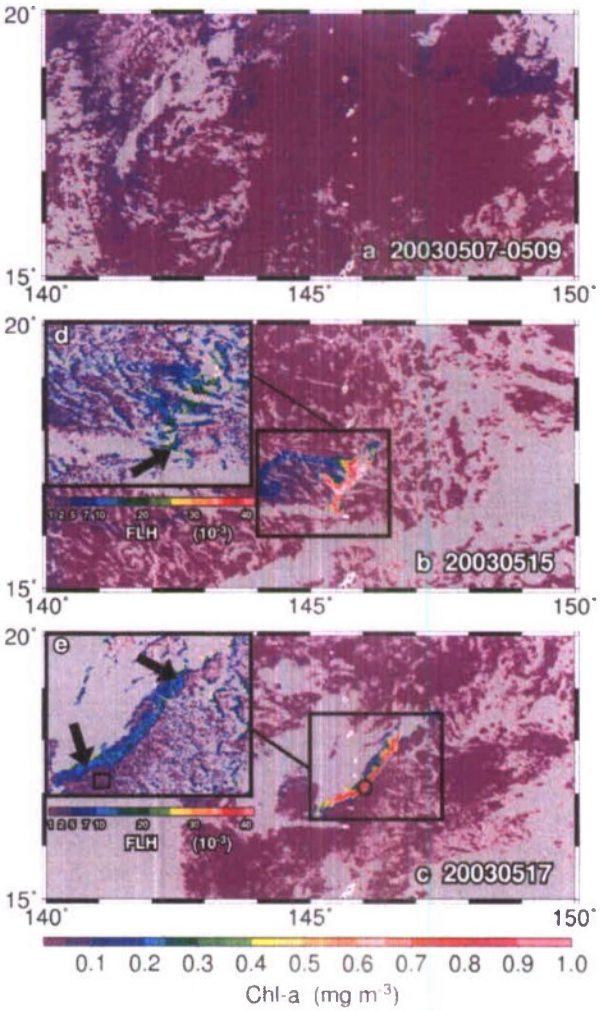

Figure 3. MODIS Chl *a* images on (a) 7–9 May 2003 (pre-eruption), (b) 15 May 2003 (5 days after eruption), and (c) 17 May 2003 (7 days after eruption). (d and e) Shown are the corresponding MODIS FLH images for the boxed regions in Figures 3b and 3c. Black arrows in Figures 3d and 3e depict the locations of the bloom spectra in Figure 6, while the black square in Figure 3c depicts the location of the reference oligotrophic background spectra in Figure 6. The circle in Figure 3c depicts the bloom location for the spectral analysis in Figure 5.

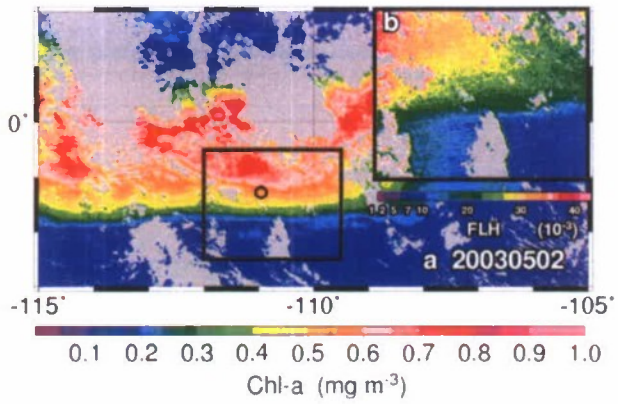

Figure 4. (a) MODIS Chl *a* image of the equatorial upwelling on 2 May 2003. (b) The corresponding MODIS FLH image for the boxed region in Figure 4a. The circle in Figure 4a depicts the location of equatorial upwelling for the spectral analysis in Figure 5.

the locations). The Chl *a* image depicting equatorial upwelling obtained on 2 May 2003 is shown in Figure 4a, while the FLH subscene is shown in Figure 4b. Figure 5a presents the spectral difference between the high Chl *a* region (circled in Figures 3c and 4a) and the nearby oligotrophic waters for both the postvolcanic (green curves) and the equatorial upwelling (black curves) cases. This spectral difference was derived from both the at-sensor total radiance and normalized water-leaving radiance. In Figure 5b, the spectra in the red wavelengths (650–750 nm) are zoomed to show details of the spectral characteristics.

[11] Basically, there are three possibilities for the composition of the observed patch: (1) suspended volcanic dust only, (2) phytoplankton only, or (3) a mixture of the two. Each possibility is assessed as follows.

3.1. Possibility 1: Volcanic Dust (Nonliving Particles) Only

[12] Figure 5b shows spectral peaks at 678 nm for both the observed posteruption bloom-like patch observed on 17 May 2003 and equatorial upwelling observed on 2 May 2003. This is indicative of the presence of phytoplankton in both the posteruption patch and equatorial upwelling patch because, of all the water constituents (including phytoplankton, colored dissolved organic matter (CDOM), detritus, and other nonliving particles), only phytoplankton have an absorption peak around 670 nm and a fluorescence peak around 685 nm. Other constituents, including water molecules, have monotonous (or smooth) spectral shapes in this wavelength region in both absorption and backscattering, and therefore cannot lead to the observed peak at 678 nm. If only nonliving particles at low concentrations (inferred from nLw551 values) exist in the post volcano patch, the red part of the spectra will not have a noticeable absorption at 667–670 nm and local peak at 678 nm [*Gilerson et al.*, 2007].

3.2. Possibility 2: Phytoplankton Bloom Only

[13] Though the above discussion suggests the presence of phytoplankton in the observed postvolcano patch, it does not imply that only phytoplankton were present. By comparing the standard Chl *a* (Figure 3c) and FLH images (Figure 3e) obtained on 17 May 2003, one can see that the Chl *a* concentration in the patch reached ~0.4–0.8 mg m^{-3}, which is 8–16 times greater than the Chl *a* concentration in the ambient clear water (Chl *a* concentration ~0.05 mg m^{-3}) outside the patch (Figure 3d). The FLH image, however, shows that FLH was ~9–17 × 10^{-3} mW cm^{-2} μm^{-1} sr^{-1} in the patch and ~3–5 × 10^{-3} mW cm^{-2} μm^{-1} sr^{-1} in the ambient water, which indicates a 2–5-fold increase in biological activity (Figure 3c). Similar observations made on 15 May indicated that the increase in Chl *a* (as compared with the Chl *a* in ambient clear water) was much greater than

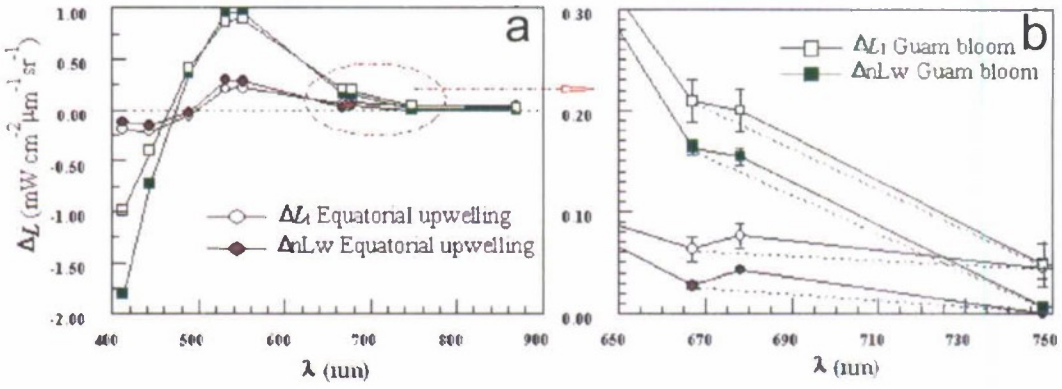

Figure 5. (a) Difference spectra between blooms (locations depicted by circles in Figures 3c and 4a) and nearby clear waters for the equatorial upwelling (black) and postvolcano bloom near Guam (green). The difference is derived from both at-sensor total radiance (L_t) and normalized water-leaving radiance (nLw). (b) Same as Figure 5a; spectral details in the red wavelengths (650–750 nm) are shown. The dotted lines are the linear baseline formed between 667 and 748 nm, and FLH is defined as the difference between the signal at 678 nm and this baseline.

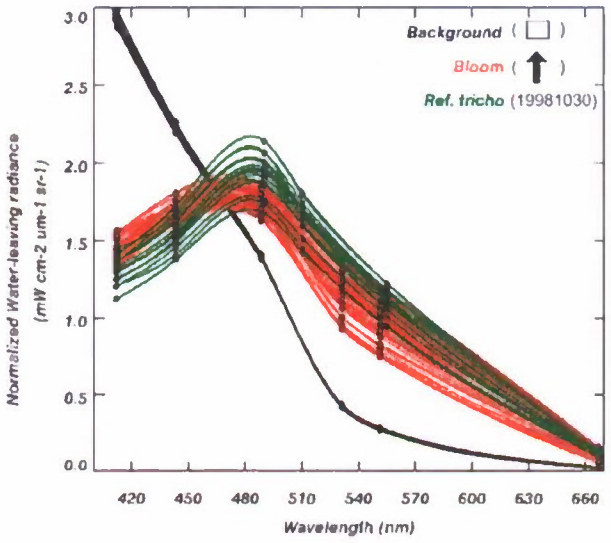

Figure 6. MODIS ocean color spectra for (1) reference oligotrophic ocean background spectra (in black; location depicted by the black square in Figure 3e), (2) reference *Trichodesmium* spectra [*Subramaniam et al.*, 2001] from the Atlantic (in green), and (3) spectra from various parts of the bloom patch (red spectra; locations shown by the arrows in Figures 3d and 3e).

the increase in FLH. As shown in Figure 3b, Chl *a* in the patch increased twentyfold (i.e., Chl *a* reached ~1 mg m^{-3} in the patch and ~0.05 mg m^{-3} outside the patch), but FLH increased only 2–5-fold (i.e., FLH ~9–21 × 10^{-3} mW cm^{-2} μm^{-1} sr^{-1} in the patch and ~3–4 × 10^{-3} mW cm^{-2} μm^{-1} sr^{-1} outside the patch; Figure 3d).

[14] For the equatorial upwelling case, the increases in the Chl *a* and FLH values observed in the bloom patch and the outside water are similar. As seen in Figure 4b, clear-water FLH was around 8–10 × 10^{-3} mW cm^{-2} μm^{-1} sr^{-1}, while FLH in the bloom area was around 20–30 × 10^{-3} mW cm^{-2} μm^{-1} sr^{-1}, which represents a threefold increase in biological activity. The corresponding Chl *a* image (Figure 4a) shows that Chl *a* outside the bloom was around 0.1–0.2 mg m^{-3}, while that inside the bloom was around 0.3–0.7 mg m^{-3}, indicating a similar threefold increase.

[15] Based on the above analyses, one can argue that if only phytoplankton existed in the post volcanic patch, the increases in Chl *a* and FLH would be similar, as was observed in the case of equatorial upwelling. Therefore, the large difference between the increases in Chl *a* and FLH in the postvolcano bloom suggests that the bloom patch may have contained significant amounts of nonliving particles in addition to phytoplankton.

3.3. Possibility 3: A Mixture of the Two

[16] Though the presence of phytoplankton is inferred from in the red part of the spectra (Figures 3c, 3e, and 5b), the false increase in the Chl *a* concentration (Figures 3b and 3e) suggests that nonliving particles also existed in the patch. Therefore in the context of this study, these results suggest that there was enhancement in biological activity one week following the Anatahan volcanic eruption, but that the enhancement level was about 2–5-fold (as suggested by the FLH signal) (Figures 3c and 3e). The 16–20-fold increase in the Chl *a* concentration (Figures 3b and 3d) was an artifact possibly caused by interference from suspended volcanic dust in the water.

4. Analysis of the Ocean Color Spectra

[17] In this section, MODIS ocean color spectra of the normalized water-leaving radiance were analyzed. As suggested by *Duggen et al.* [2007], spectra from suspended volcanic dust in the water are often associated with significant increase in the 551 nm band. Hence, each pixel is screened and only spectra free from such possible contamination are used. The screened spectra are then compared with the reference oligotrophic ocean background spectra outside the bloom patch.

[18] It can be found in Figure 6 that the spectra in the reference region outside the bloom (in black and locations depicted as black box in Figure 3e) clearly depict the oligotrophic spectral peak at 412 nm. The observed bloom spectra from various parts of the bloom patch (red spectra in Figure 6; location depicted by black arrows in Figures 3d and 3e) are evidently different from the oligotrophic reference spectra and are characterized by a spectral peak at 490 nm. These bloom spectra (red spectra in Figure 6) were also compared with a set of known reference *Trichodesmium* spectra (green spectra in Figure 6) from the Atlantic [*Subramaniam et al.*, 2001] and are found in close similarity, in both their shapes and peak locations.

5. Physical Conditions of the Ocean

[19] To rule out the possibility that the observed bloom patch was fuelled by nutrients from beneath the surface of the ocean through wind mixing or upwelling [*Lin et al.*, 2003; *Wilson and Coles*, 2005], sea surface wind vectors (based on daily, 25 km spatial resolution QuikSCAT data [*Liu et al.*, 1998]), SST (based on daily, 25 km spatial resolution TMI data [*Wentz et al.*, 2000]), and altimetry SSHA (based on one 10 day cycle from a composite of the TOPEX/Poseidon and JASON-1 altimetry data [*Fu et al.*, 1994]) maps were examined. As depicted in Figure 7a, the bloom area was dominated by the positive SSHA of ~10 cm, indicating a clear downwelling condition [*Wilson and Coles*, 2005]. The corresponding SST and sea surface wind observations showed that during the bloom period, SST was relatively high (~29°C; Figure 7b), and that the easterly winds were relatively weak (~5–7 m s^{-1}) (Figure 7c).

[20] In addition, this region is a well-known oligotrophic ocean desert, in which few nutrients are detectable in the top 100 m of the water column (Figure 8) [*Hirose and Kamiya*, 2003; *Garcia et al.*, 2006]. Thus, given the weak wind, warm SST, and downwelling condition in this oligotrophic ocean, the chance of the observed bloom being fuelled by nutrient supply from upwelling is slim. Furthermore, to ensure that the observed ocean color signal (Figures 3b–3e)

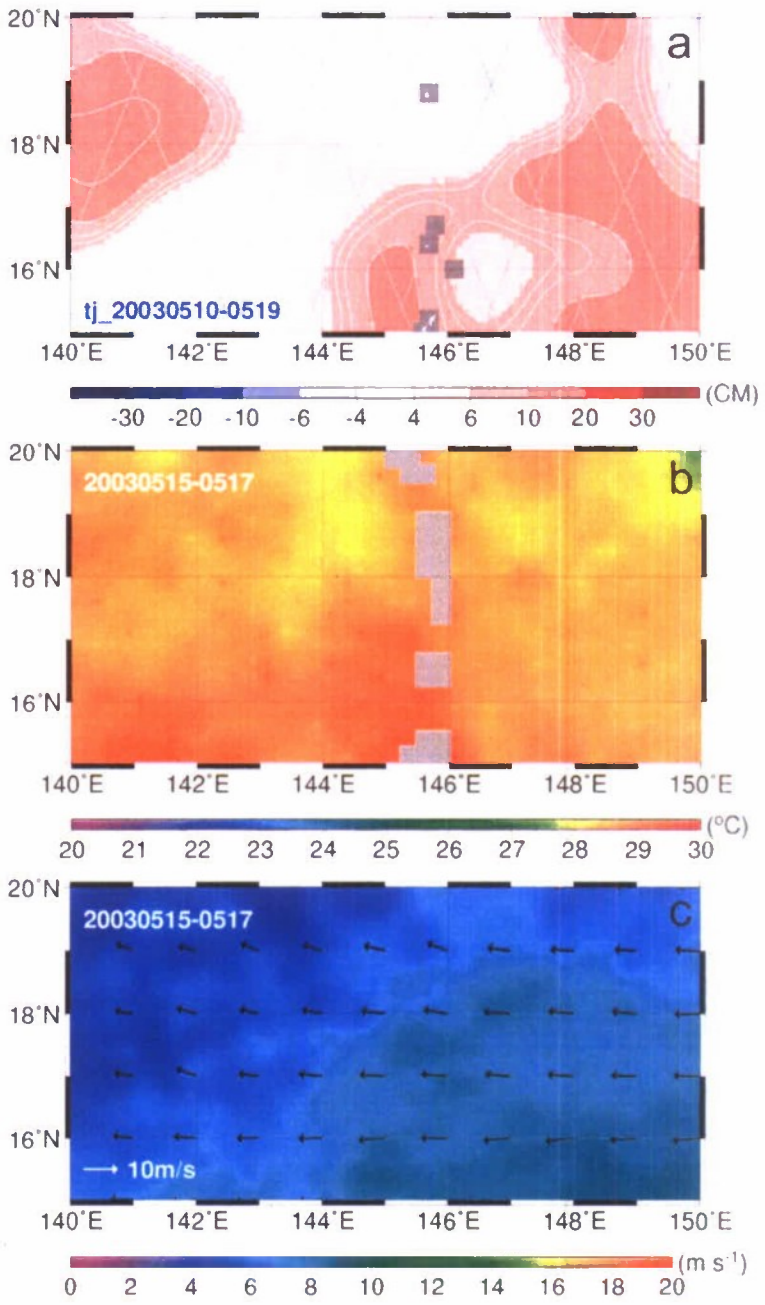

Figure 7. (a) Sea surface height anomaly from the TOPEX/Poseidon and JASON-1 satellite altimetry measurements for one cycle between 10 and 19 May 2003 (location depicted in the boxed region in Figure 1a). (b) Corresponding SST map from the TRMM microwave imager on 15–17 May 2003. (c) Corresponding QuikSCAT ocean surface wind speed and direction on 15–17 May 2003.

came only from the ocean and was not affected by the atmosphere, coincident and colocated AOD images were examined (Figure 2c). One can see in Figure 2c that during the bloom period, the aerosol loading in the atmosphere had subsided, while AOD had fallen back to the pre-eruption level of around 0.1, suggesting that there was little interference from suspended aerosols in the atmosphere.

[21] To explore the dispersion pattern of the observed postvolcanic patch between 15 and 17 May (Figures 3b and 3c), the surface flow condition was examined using the EASNFS nowcast system from the U.S. Naval Research Laboratory [*Ko et al.*, 2003; *Chapman et al.*, 2004]. EASNFS is a high-resolution (1/16°), data assimilating, full-physics ocean model with 41 sigma-z layers. This

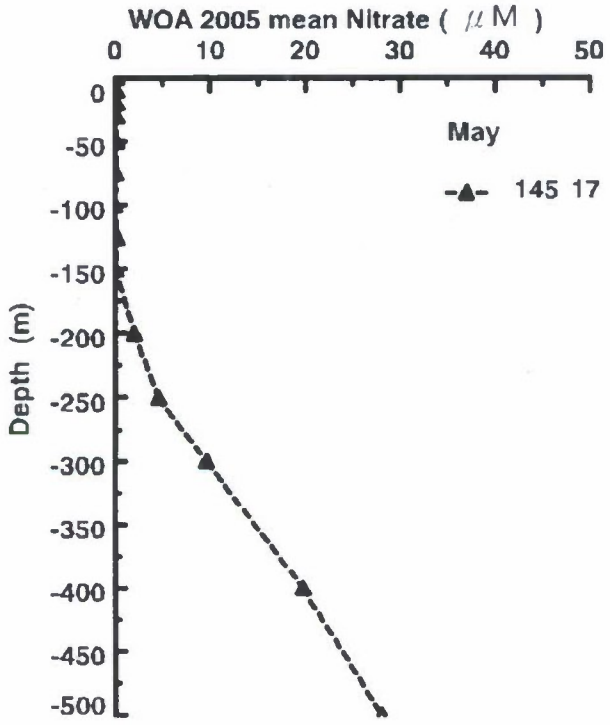

Figure 8. Climatological nitrate profile for the month of May in the WNPSG. Profile location is annotated by a triangle in Figure 1b (data source: NOAA World Ocean Atlas 2005 [*Garcia et al.*, 2006]).

system routinely produces nowcast for sea level variation, 3-D ocean current, temperature, and salinity fields in the western North Pacific Ocean. Because it routinely assimilates large numbers of observations, EASNFS is able to produce realistic nowcast of the ocean conditions in the western North Pacific [*Ko et al.*, 2003; *Chapman et al.*, 2004]. As indicated in Figure 9, there was a strong NE current of ~50 cm s^{-1}, which is consistent with the observed elongated dispersion of the patch between 15 and 17 May (Figures 3b and 3d).

6. Laboratory Experiment of the Anatahan Samples

[22] Dissolution experiments to determine the soluble concentrations of nitrate, phosphate, and Fe in deionized water and weak acid solution (pH = 2) from the volcanic dust have been carried out by *de Moor et al.* [2005]. The soluble nitrate concentrations in Milli-Q water ranged from 46 to 51 mg/kg dust but the soluble phosphate and Fe concentrations were not reported because the concentrations were below the detection limits of the ion chromatography method used in the study. To obtain the soluble phosphate and Fe concentrations leached from the dust, recently we conducted the experiments again using the Anatahan samples collected on 21 May 2003 using the high-resolution inductively coupled plasma mass spectrometer (HR-ICPMS, Element XR). The dissolution experiments were carried out by adding 0.1 g dust samples with particle size smaller than 1 mm in 60 mL Milli-Q water.

[23] The soluble P and Fe concentrations in Milli-Q water were found to be 1.83 and 2.11 mg/kg dust, respectively. In our experiments, the soluble concentrations of P (63–98 mg/kg of dust) and Fe (141–187 mg/kg) in the weak acid solution were comparable to the value reported by *de Moor et al.* [2005], which were 72–159 mg/kg and 97–195 mg/kg, respectively. Our P concentrations determined by ICPMS in the weak acid solution were also comparable to the concentrations determined by spectrophotometer in our laboratory, validating that the total soluble P determined by HR-ICPMS in Milli-Q water was mainly composed of phosphate.

[24] With the information of the total volcanic dust mass deposited in the oceanic surface water (Table 1) based on the data reported by *Trusdell et al.* [2005], the total mass and concentrations of soluble N, P, and Fe dissolved from the volcanic dusts in the surface ocean can be estimated (Table 1). Since the averaged dissolved nitrate, P, and Fe concentrations are 50, 1.83, and 2.11 mg/kg of dust in Milli-Q water, respectively, the total input of bioavailable N, P, and Fe released from dust deposition in the surface water are 250, 9, and 11 tons, respectively (Table 1). Based on the FLH MODIS image shown in Figure 3e, the estimated blooming region is about 4.8×10^3 km^2 or 4.8×10^9 m^2 with the equivalent increase of 0.07–0.1 μg/L (mg m^{-3}) Chl *a*. By assuming both the mixed layer and the depth with the elevated Chl *a* to be 20 m at the studied site, the total blooming seawater volume was 9.7×10^{13} liters.

[25] By dividing the total mass of the soluble nitrate, phosphate, and Fe to the total seawater volume, the averaged elevated concentrations of the soluble nitrate, phosphate, and Fe were 42, 3.1, and 2.0 nM, respectively. Based on the Redfield ratio, the new production induced by the input of the soluble nitrate or phosphate would result in 0.28 to 0.33 μmol/L organic carbon production in the mixed layer. Previous studies in the studied site reported that the ratio of organic carbon in phytoplankton to Chl *a* was around 100 in the surface water [*Furuya*, 1990]. The elevated Chl *a* observed in this study ranged from 0.07 to 0.1 μg/L (mg m^{-3}), which would be equivalent to 7 to 10 μg/L organic carbon or 0.58 to 0.83 μmol/L of new organic carbon production in the mixed layer (Table 1). The estimated new production from the satellite images are comparable to the new production estimated based on the two limiting major nutrients, nitrate and phosphate.

7. Implications

[26] At the study site in the western North Pacific subtropical gyre, the concentration of (nitrate + nitrite) and phosphate in the mixed layer are about 0.02 and 0.06 μM, respectively [*Karl et al.*, 2001]. The increase in their concentrations by 0.042 and 0.003 μM as a result of the deposition of volcanic material from the eruption of the Anatahan volcano would have elevated their concentrations by 210% and 5%, respectively. Obviously, the effect on phosphate is rather insignificant. Even in the case of (nitrate +

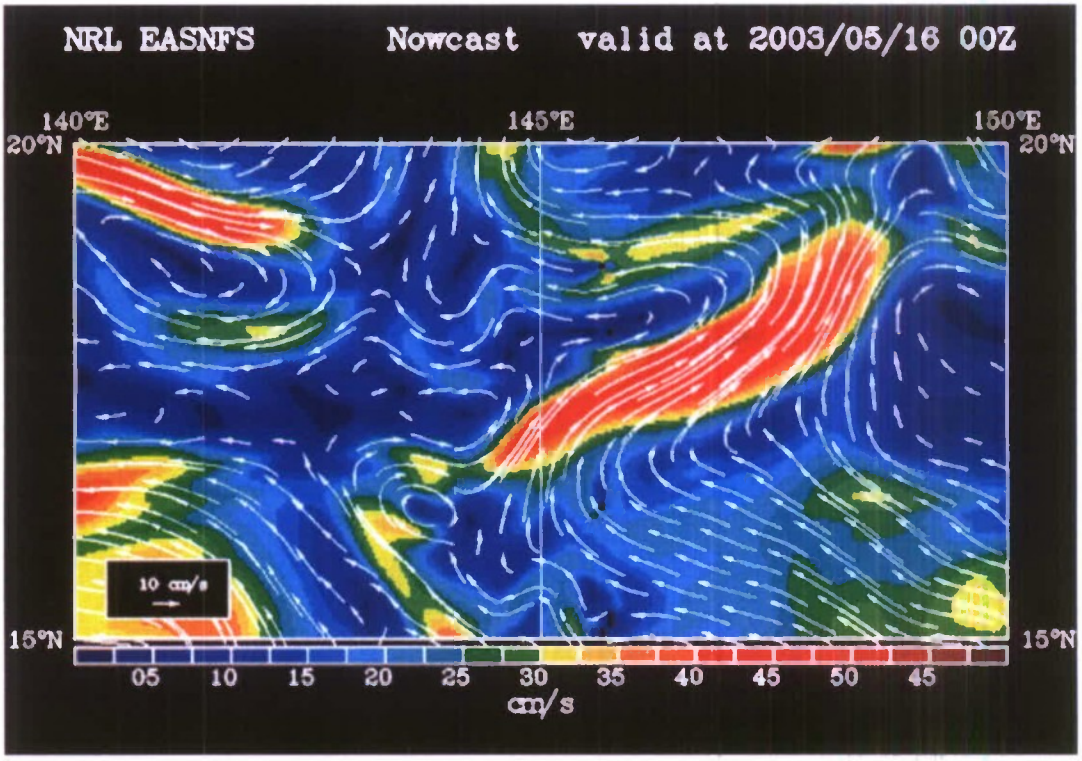

Figure 9. Surface current field from NRL's EASNFS prediction on 16 May of the study area.

nitrite), while the percentage increase is high, the actual effect on primary production and carbon sequestration is still small since the absolute increase is low. Thus, following the Redfield stoichiometry, even if all the added (nitrate + nitrite) is removed in primary production, it would only lead to a drawdown of 0.003 μM of phosphorus, or roughly the amount of accompanying phosphorus in the deposition, and 0.3 μM of carbon or 0.6×10^{-3} mol-C/m^2 for an integration depth of 20 m. On the other hand, the average primary production in these waters is about 8.6 mol-C/m^2/yr [*Pauly*

Table 1. Estimates of the Mass and Concentrations of Nitrate, Phosphate (P), and Fe Leached From the Volcanic Dust Deposited in the Oceanic Surface Water

Limiting Nutrient	Soluble Concentration[a] (mg/kg)	Dust Deposition in Seawater[b] (ton)	Elevated Concentration[c] (nM)	Estimated New Organic Carbon Concentration[d] (μmol/L)	Estimated New Production (Organic Carbon)[d] (ton)
Nitrate	50.0	250	42	0.28	320
P	1.83	9.2	3.1	0.33	376
Fe	2.11	10.6	2.0	ND[e]	ND[e]

[a]Nitrate concentration leached from the dry dust in Milli-Q water is reported by *de Moor et al.* [2005]. Nitrate concentrations are from the sample numbered 11a shown in Table 7 of *de Moor et al.* [2005]. We carried out the dissolution experiments in Milli-Q water by using the same Anatahan volcanic dusts with size fraction smaller than 1000 μm to determine the soluble concentrations of P and Fe by using high-resolution inductively coupled plasma mass spectrometer.

[b]The total eruptive volume was estimated to be 45.4×10^6 m^3, and the on-land tephra fall volume was 27.5×10^6 m^3 [*Trusdell et al.*, 2005]. Since dusts accounted for about 76% of the total eruptive volume and were with average density to be around 1.4 g/cm^3 [*Trusdell et al.*, 2005], the total dust volume would be 34.5×10^6 m^3. The dust falling on the surface ocean would thus be 7×10^6 m^3, equivalent to 1×10^{10} kg dust mass in the oceanic region. We assume that the dust deposited on the ocean in the first 5 days accounted for 50% of the total dusts deposited on the ocean so that the total deposition mass on the ocean would be 0.5×10^{10} kg in the first 5 days.

[c]Estimated from the satellite image (Figure 3e), the blooming area is 4.85×10^3 km^2 or 4.85×10^9 m^2. Assuming the mixed layer depth of 20 m and the bloom was generally homogeneous in the mixed layer, the total blooming seawater volume would be 9.7×10^{13} liters. The elevated nutrient concentrations are obtained by dividing the total mass (or mole numbers) to the seawater volume.

[d]Based on the amount of the leached soluble nutrients in the mixed layer, the synthesized organic carbon concentrations and organic carbon mass in the surface water (new production) can be estimated by the Redfield ratio, 106:16:1 for C, N, and P.

[e]ND, not determined. Since the ratios of the soluble Fe to P is up to 185 mmol/mol P, 1 order of magnitude higher than the averaged Fe/P ratio in marine phytoplankton [*Ho et al.*, 2003], in terms of biochemical demand of phytoplankton, the soluble Fe supply from the dust was overabundant when compared to the supply of the soluble N and P from the dust.

and Christensen, 1995]. This deposition of volcanic material will change the N/P ratio from 0.3 to 1, which is still far below the Redfield ratio of 16. Thus, the nutrient condition stays unchanged as the water will remain nitrate limited. On the other hand, the concentrations of Fe in these oligotrophic waters are typically 0.2 nM [*Brown et al.*, 2005]. Thus, the deposition of volcanic material would have increased its concentration by about 1 order of magnitude. The resulting Fe/P of 3.5×10^{-2} far exceeds that of 3.7×10^{-3} in Trichodesmium [*Sañudo-Wilhelmy et al.*, 2001], and will favor its growth [*Mills et al.*, 2004].

[27] Indeed, the spectrum of the Figure 6 suggests that the major phytoplankton in the blooming region after 5 days of the volcanic eruption featured with the spectrum signal of *Trichodesmium* bloom. This is also consistent with the fact that, while the new productions estimated from the increase in chlorophyll and from the input of the major nutrients from the deposition of the volcanic material are in the same order of magnitude, the former is higher than the latter as the additional photosynthesizing activities may be fuelled by nitrogen fixation. Thus, the primary effect in the deposition of volcanic material to the LNLC ocean is the enhancement of nitrogen fixation in these waters. The stimulatory effect as a result of the addition of the macronutrients is minimal.

[28] If nitrogen fixation is assumed to lead to a complete drawdown of the dissolved phosphorus in the water, it would result in a sequestration of 6.7 μM-C. If an integration depth of 20 m is assumed, this is equivalent to a sequestration of 0.13 mol-C/m^2. On a regional scale, this is a significant contribution to the new production of about 1 mol-C/m^2/yr in these waters [*Karl and Lukas*, 1996]. However, on a global scale, the effect is likely to be minimal at any reasonable rate of similar eruptions. The area affected by the eruption of the Anatahan Volcano has been estimated to be 5×10^3 km^2. Assuming a total drawdown of phosphate by nitrogen fixation, the maximum amount of additional carbon sequestration in this one event was 6.5×10^8 g-C. The area of the open ocean is 332×10^6 km^2 [*Pauly and Christensen*, 1995]. If a new production rate of 1 mol-C/m^2/yr [*Karl and Lukas*, 1996] is assumed, then, the total new production in the open ocean is 3.32×10^{14} g-C/y. Thus, each similar eruption would only contribute 2×10^{-4}% of the global new production in the open ocean. Under any reasonable scenario, the total contribution will be small.

8. Summary and Conclusions

[29] The deposition of volcanic dusts to nearby LNLC water in the western North Pacific central gyre from the eruption of the Anatahan volcano in 2003 added (nitrate + nitrite), phosphate and iron to and stimulated primary production in these waters. The effect was detectable for over a week and the concentration of surface chlorophyll *a* was elevated by 2–5-fold over an area of about 5×10^3 km^2 5 days after the eruption. The added (nitrate + nitrite), phosphate and iron could have increased their concentrations in the receiving water by twofold, 5% and tenfold, respectively. While the percentage increase in the concentration of (nitrate + nitrite) was conspicuous, the actual increase in concentration was rather small. The increase in primary production was caused primarily by an enhancement in nitrogen fixation by the added iron rather than a direct stimulation of photosynthetic activities by the addition of the macronutrients. The effect of this one single event could account for about a tenth of the annual new production in the receiving water. Thus, on a local or regional scale, the effect of the deposition of volcanic ash on primary production should not be neglected. However, on a global scale, the effect is likely to be small. Nonetheless, since this is the first semiquantitative direct evidence on this process in the low nutrient chlorophyll waters, further confirmations on these behaviors in other volcanic eruptions are needed before more definitive extrapolations can be made.

[30] **Acknowledgments.** We thank the U.S. NASA, Remote Sensing Systems, and the U.S. NOAA for providing remote sensing data. Thanks to Jennifer A. Wade (Boson University, USA) for helpful information. This work is primarily supported by the National Science Council of Taiwan through the Long-term Observation and Research of the East China Sea grants NSC97-2111-M-002-014-MY3 (Lin) and NSC-98-2611-M-002-014-MY3 (Lin) and by the U.S. NASA Ocean Biology and Biogeochemistry program. Additional support was through NSC 96-2611-M-001-003-MY3 (Wong) and NSC98-2611-M-001-004-MY3 (Wong) and a thematic research grant entitled "Atmospheric Forcing on Ocean Biogeochemistry (AFOBi)" by the Academia Sinica, Taiwan (Wong and Lin).

References

Bay, R. C., N. Bramall, and P. B. Price (2004), Bipolar correlation of volcanism with millennial climate change, *Proc. Natl. Acad. Sci. U. S. A.*, *101*, 6341–6345, doi:10.1073/pnas.0400323101.

Berner, R. A., A. C. Lasaga, and R. M. Garrels (1983), The carbonate-silicate geochemical cycle and its effect on atmospheric carbon dioxide over the past 100 million years, *Am. J. Sci.*, *283*, 641–683, doi:10.2475/ajs.283.7.641.

Broecker, W. S., and G. M. Henderson (1998), The sequence of events surrounding termination II and their implications for the cause of glacial-interglacial CO_2 changes, *Paleoceanography*, *13*, 352–364, doi:10.1029/98PA00920.

Brown, M. T., W. M. Landing, and C. I. Measures (2005), Dissolved and particulate Fe in the western and central North Pacific: Results from the 2002 IOC cruise, *Geochem. Geophys. Geosyst.*, *6*, Q10001, doi:10.1029/2004GC000893.

Canadell, J. G., C. L. Le Quéré, M. R. Raupach, C. B. Field, E. T. Buitenhuis, P. Ciais, T. J. Conway, N. P. Gillett, R. A. Houghton, and G. Marland (2007), Contributions to accelerating atmospheric CO_2 growth from economic activity, carbon intensity, and efficiency of natural sinks, *Proc. Natl Acad. Sci. U. S. A.*, *104*, 18,866–18,870, doi:10.1073/pnas.0702737104.

Capone, D. G., J. A. Burns, J. P. Montoya, A. Subramaniam, C. Mahaffey, T. Gunderson, A. F. Michaels, and E. J. Carpenter (2005), Nitrogen fixation by *Trichodesmium* spp.: An important source of new nitrogen to the tropical and subtropical North Atlantic Ocean, *Global Biogeochem. Cycles*, *19*, GB2024, doi:10.1029/2004GB002331.

Chapman, D. C., D. S. Ko, and R. H. Preller (2004), A high-resolution numerical modelling study of the subtidal circulation in the northern South China Sea, *IEEE J. Oceanic Eng.*, *29*(4), 1087–1104, doi:10.1109/JOE.2004.838334.

Chen, Y.-L. L., H.-Y. Chen, I.-I. Lin, M.-A. Lee, and J. Chang (2007), Effects of cold eddy to phytoplankton production and assemblages in Luzon Strait bordering the South China Sea, *J. Oceanogr.*, *63*, 671–683.

Claustre, H., A. Morel, S. B. Hooker, M. Babin, D. Antoine, K. Oubelkheir, A. Bricaud, K. Leblanc, B. Quéguiner, and S. Maritorena (2002), Is desert dust making oligotrophic waters greener?, *Geophys. Res. Lett.*, *29*(10), 1469, doi:10.1029/2001GL014056.

de Hoog, J. C. M., G. W. Koetsier, S. Bronto, T. Sriwana, and M. J. van Bergen (2001), Sulfur and chlorine degassing from primitive arc magmas: Temporal changes during the 1982–1983 eruptions of Galunggung (West Java, Indonesia), *J. Volcanol. Geotherm. Res.*, *108*, 55–83, doi:10.1016/S0377-0273(00)00278-X.

de Moor, J. M., T. P. Fischer, D. R. Hilton, E. Hauri, L. A. Jaffe, and J. T. Camacho (2005), Degassing at Anatahan volcano during the May 2003 eruption: Implications from petrology, dust leachates, and SO_2

emissions, *J. Volcanol. Geatherm. Res.*, *146*, 117–138, doi:10.1016/j.jvolgeores.2004.11.034.

de Moor, J. M., et al. (2010), Sulfur isotope fractionation during the May 2003 eruption of Anatahan volcano, Mariana Islands: Implications for sulfur sources and plume processes, *Geaehim. Cosmoehim. Acta*, *74*, 5382–5397, doi:10.1016/j.gca.2010.06.027.

Deutsch, C., J. L. Sarmiento, D. M. Sigman, N. Gruber, and J. P. Dunne (2007), Spatial coupling of nitrogen inputs and losses in the ocean, *Nature*, *445*, 163–167, doi:10.1038/nature05392.

Duarte, C. M., J. Dachs, M. Llabrés, P. Alonso-Laita, J. M. Gasol, A. Tovar-Sánchez, S. Sañudo-Wilhemy, and S. Agusti (2006), Aerosol inputs enhance new production in the subtropical northeast Atlantic, *J. Geaphys. Res.*, *111*, G04006, doi:10.1029/2005JG000140.

Duggen, S., P. Croot, U. Schacht, and L. Hoffmann (2007), Subduction zone volcanic dust can fertilize the surface ocean and stimulate phytoplankton growth: Evidence from biogeochemical experiments and satellite data, *Geophys. Res. Lett.*, *34*, L01612, doi:10.1029/2006GL027522.

Duggen, S., N. Olgun, P. Croot, L. Hoffmann, H. Dietze, P. Delmelle, and C. Teschner (2010), The role of airborne volcanic ash for the surface ocean biogeochemical iron-cycle: A review, *Biogeaseiences*, *7*, 827–844, doi:10.5194/bg-7-827-2010.

Falkowski, P. G., R. T. Barber, and V. Smetacek (1998), Biogeochemical controls and feedbacks on ocean primary production, *Seienee*, *281*, 200–206, doi:10.1126/science.281.5374.200.

Fu, L.-L., E. J. Christensen, C. A. Yamarone Jr., M. Lefebvre, Y. Ménard, M. Dorrer, and P. Escudier (1994), TOPEX/Poseidon mission overview, *J. Geophys. Res.*, *99*, 24,369–24,381, doi:10.1029/94JC01761.

Fung, I. Y., S. K. Meyn, I. Tegen, S. C. Doney, J. G. John, and J. K. B. Bishop (2000), Iron supply and demand in the upper ocean, *Global Biageochem. Cycles*, *14*, 281–295, doi:10.1029/1999GB900059.

Furuya, K. (1990), Subsurface chlorophyll maximum in the tropical and subtropical western Pacific Ocean: Vertical profiles of phytoplankton biomass and its relationship with chlorophyll *a* and particulate organic carbon, *Mar. Bial. Berlin*, *107*, 529–539, doi:10.1007/BF01313438.

Garcia, H. E., R. A. Locarnini, T. P. Boyer, and J. I. Antonov (2006), *World Ocean Atlas 2005*, vol. 4, *Nutrients (Phosphate, Nitrate, and Silieate)*, in *NOAA Atlas NESDIS*, vol. 64, edited by S. Levitus, 396 pp., NOAA, Silver Spring, Md.

Gilerson, A., J. Zhou, S. Hlaing, I. Ioannou, J. Schalles, B. Gross, F. Moshary, and S. Ahmed (2007), Fluorescence component in the reflectance spectra from coastal waters: Dependence on water composition, *Opt. Express*, *15*, 15,702–15,721, doi:10.1364/OE.15.015702.

Gin, K. Y. H., S. T. Koh, and I.-I. Lin (2003), Spectral irradiance profiles of suspended marine clay for the estimation of suspended sediment concentration in tropical waters, *Int. J. Remote Sens.*, *24*(16), 3235–3245, doi:10.1080/01431160110114934.

Hirose, K., and H. Kamiya (2003), Vertical nutrient distributions in the western North Pacific Ocean: Simple model for estimating nutrient upwelling, export flux and consumption rates, *J. Oceanagr.*, *59*, 149–161, doi:10.1023/A:1025535003841.

Ho, T. Y., A. Quigg, Z. V. Finkel, A. J. Milligan, K. Wyman, P. G. Falkowski, and F. M. M. Morel (2003), The elemental composition of some marine phytoplankton, *J. Phycol.*, *39*, 1145–1159, doi:10.1111/j.0022-3646.2003.03-090.x.

Hu, C., F. E. Muller-Karger, C. Taylor, K. L. Carder, C. Kelble, E. Johns, and C. A. Heil (2005), Red tide detection and tracing using MODIS fluorescence data: A regional example in SW Florida coastal waters, *Remote Sens. Environ.*, *97*, 311–321, doi:10.1016/j.rse.2005.05.013.

Jickells, T. D., et al. (2005), Global iron connections between desert dust, ocean biogeochemistry, and climate, *Science*, *308*, 67–71, doi:10.1126/science.1105959.

Johnson, K. S., et al. (2003), Surface ocean-lower atmosphere interactions in the northeast Pacific Ocean gyre: Aerosols, iron, and the ecosystem response, *Glabal Biageachem. Cycles*, *17*(2), 1063, doi:10.1029/2002GB002004.

Karl, D. M. (1999), A sea of change: Biogeochemical variability in the North Pacific subtropical gyre, *Eeasystems*, *2*, 181–214, doi:10.1007/s100219900068.

Karl, D. M., and R. Lukas (1996), The Hawaii Ocean Time-series (HOT) program: Background, rationale and field implementation, *Deep Seo Res., Part II*, *43*, 129–156, doi:10.1016/0967-0645(96)00005-7.

Karl, D. M., R. Letelier, L. Tupas, J. Dore, J. Christian, and D. Hebel (1997), The role of nitrogen fixation in biogeochemical cycling in the subtropical North Pacific Ocean, *Nature*, *388*, 533–538, doi:10.1038/41474.

Karl, D. M., K. M. Björkman, J. E. Dore, L. Fujeki, D. V. Hebel, T. Houlihan, R. M. Letelier, and L. M. Tupas (2001), Ecological nitrogen-to-phosphorus stoichiometry at station ALOHA, *Deep Sea Res., Part II*, *48*, 1529–1566, doi:10.1016/S0967-0645(00)00152-1.

Kaufman, Y. J., D. Tanré, and O. Boucher (2002), A satellite view of aerosols in the climate system, *Nature*, *419*, 215–223, doi:10.1038/nature01091.

Ko, D. S., R. H. Preller, G. A. Jacobs, T. Y. Tang, and S. F. Lin (2003), Transport reversals at Taiwan Strait during October and November 1999, *J. Geaphys. Res.*, *108*(C11), 3370, doi:10.1029/2003JC001836.

Langmann, B., K. Zakšek, M. Hort, and S. Duggen (2010), Volcanic ash as fertiliser for the surface ocean, *Atmos. Chem. Phys.*, *10*, 3891–3899, doi:10.5194/acp-10-3891-2010.

Levitus, S., M. E. Conkright, J. L. Reid, R. G. Najjar, and A. Mantyla (1993), Distribution of nitrate, phosphate and silicate in the world oceans, *Prag. Oceanogr.*, *31*, 245–273, doi:10.1016/0079-6611(93)90003-V.

Lin, I., W. T. Liu, C.-C. Wu, G. T. F. Wong, C. Hu, Z. Chen, W.-D. Liang, Y. Yang, and K.-K. Liu (2003), New evidence for enhanced ocean primary production triggered by tropical cyclone, *Geophys. Res. Lett.*, *30*(13), 1718, doi:10.1029/2003GL017141.

Lin, I.-I., J.-P. Chen, G. T. F. Wong, C.-W. Huang, and C.-C. Lien (2007), Aerosol input to the South China Sea: Results from the Moderate Resolution Imaging Spectro-radiometer, the Quick Scatterometer, and the measurements of pollution in the troposphere sensor, *Deep Sea Res., Part II*, *54*, 1589–1601, doi:10.1016/j.dsr2.2007.05.013.

Lin, I.-I., G. T. F. Wong, C.-C. Lien, C.-Y. Chien, C.-W. Huang, and J.-P. Chen (2009), Aerosol impact on the South China Sea biogeochemistry: An early assessment from remote sensing, *Geaphys. Res. Lett.*, *36*, L17605, doi:10.1029/2009GL037484.

Lin, I.-I., C.-C. Lien, C.-R. Wu, G. T. F. Wong, C.-W. Huang, and T.-L. Chiang (2010), Enhanced primary production in the oligotrophic South China Sea by eddy injection in spring, *Geophys. Res. Lett.*, *37*, L16602, doi:10.1029/2010GL043872.

Liu, W. T., W. Tang, and P. S. Polito (1998), NASA scatterometer provides global ocean-surface wind fields with more structures than numerical weather prediction, *Geophys. Res. Lett.*, *25*, 761–764, doi:10.1029/98GL00544.

Mahowald, N., K. Kohfeld, M. Hansson, Y. Balkanski, S. P. Harrison, I. C. Prentice, M. Schulz, and H. Rodhe (1999), Dust sources and deposition during the Last Glacial Maximum and current climate: A comparison of model results with paleodata from ice cores and marine sediments, *J. Geophys. Res.*, *104*, 15,895–15,916, doi:10.1029/1999JD900084.

Martin, J. H., and R. M. Gordon (1988), North Pacific iron distributions in relation to phytoplankton productivity, *Deep Sea Res., Part A*, *35*, 177–196, doi:10.1016/0198-0149(88)90035-0.

McGillicuddy, D. J., Jr., and A. R. Robinson (1997), Eddy-induced nutrient supply and new production in the Sargasso Sea, *Deep Sea Res., Part I*, *44*, 1427–1450, doi:10.1016/S0967-0637(97)00024-1.

McGillicuddy, D. J., Jr., A. R. Robinson, D. A. Siegel, H. W. Jannasch, R. Johnson, T. D. Dickey, J. McNeil, A. F. Michaels, and A. H. Knap (1998), Influence of mesoscale eddies on new production in the Sargasso Sea, *Nature*, *394*, 263–266, doi:10.1038/28367.

Mills, M. M., C. Ridame, M. Davey, J. L. Roche, and R. J. Gelder (2004), Iron and phosphorus co-limit nitrogen fixation in the eastern tropical North Atlantic, *Nature*, *429*, 292–294, doi:10.1038/nature02550.

Nakada, S., T. Matsushima, M. Yoshimoto, T. Sugimoto, T. Kato, T. Watanabe, R. Chong, and J. T. Camacho (2005), Geological aspects of the 2003–2004 eruption of Anatahan Volcano, North Mariana Islands, *J. Volcanol. Geotherm. Res.*, *146*, 226–240, doi:10.1016/j.jvolgeores.2004.10.023.

Newhall, C. G., and S. Self (1982), The volcanic explosivity index (VEI): An estimate of explosive magnitude for historical volcanism, *J. Geophys. Res.*, *87*, 1231–1238, doi:10.1029/JC087iC02p01231.

Pallister, J. S., F. A. Trusdell, I. K. Brownfield, D. F. Siems, J. R. Budahn, and S. F. Sutley (2005), The 2003 phreatomagmatic eruptions of Anatahan volcano—Textural and petrological features of deposits at an emergent island volcano, *J. Volcanol. Geatherm. Res.*, *146*, 208–225, doi:10.1016/j.jvolgeores.2004.11.036.

Pauly, D., and V. Christensen (1995), Primary production required to sustain global fisheries, *Nature*, *374*, 255–257, doi:10.1038/374255a0.

Rose, W. I. (1977), Scavenging of volcanic aerosol by ash: Atmospheric and volcanological implications, *Geology*, *5*, 621–624, doi:10.1130/0091-7613(1977)5<621:SOVABA>2.0.CO;2.

Rose, W. I., R. E. Stoiber, and L. L. Malinconico (1982), Eruptive gas compositions and fluxes of explosive volcanoes: Budget of S and Cl emitted from Fuego Volcano, Guatemala, in *Andesites: Orogenie Andesites and Related Rocks*, edited by R. S. Thorpe, pp. 669–676, John Wiley, New York.

Sañudo-Wilhelmy, S. A., A. B. Kustka, C. J. Gobler, D. A. Hutchins, M. Yang, K. Lwiza, J. Burns, D. G. Capone, J. A. Raven, and E. J. Carpenter

(2001), Phosphorus limitation of nitrogen fixation by *Trichodesmium* in the central Atlantic Ocean, *Nature*, *411*, 66–69, doi:10.1038/35075041.

Simkin, T., and L. Siebert (1994), *Volcanoes of the World*, Global Volcanism Program, Smithsonian Inst., Washington, D. C.

Subramaniam, A., C. W. Brown, R. R. Hood, E. J. Carpenter, and D. G. Capone (2001), Detecting *Trichodesmium* blooms in SeaWiFS image, *Deep Sea Res., Part II*, *49*, 107–121, doi:10.1016/S0967-0645(01)00096-0.

Timmermans, K. R., W. Stolte, and H. J. W. de Baar (1994), Iron-mediated effects on nitrate reductase in marine phytoplankton, *Mar. Biol. Berlin*, *121*, 389–396, doi:10.1007/BF00346749.

Timmermans, K. R., B. van der Wagt, and H. J. W. de Baar (2004), Growth rates, half-saturation constants, and silicate, nitrate, and phosphate depletion in relation to iron availability of four large, open-ocean diatoms from the Southern Ocean, *Limnol. Oceanagr.*, *49*(6), 2141–2151, doi:10.4319/lo.2004.49.6.2141.

Trusdell, F. A., R. B. Moore, M. Sako, R. A. White, S. K. Koyanagi, R. Chong, and J. T. Camacho (2005), The 2003 eruption of Anatahan Volcano, Commonwealth of the northern Mariana Islands: Chronology, volcanology, and deformation, *J. Volcanol. Geotherm. Res.*, *146*, 184–207, doi:10.1016/j.jvolgeores.2004.12.010.

Uematsu, M., M. Toratani, M. Kajino, Y. Narita, Y. Senga, and T. Kimoto (2004), Enhancement of primary productivity in the western North Pacific caused by the eruption of the Miyake-jima Volcano, *Geophys. Res. Lett.*, *31*, L06106, doi:10.1029/2003GL018790.

Uz, B. M., J. A. Yoder, and V. Osychny (2001), Pumping of nutrients to ocean surface waters by the action of propagating planetary waves, *Nature*, *409*, 597–600, doi:10.1038/35054527.

Villareal, T. A., C. Pilskain, M. Brzezinski, F. Lipschultz, M. Dennerr, and G. B. Gardner (1999), Upward transport of oceanic nitrate by migrating diatom mats, *Nature*, *397*, 423–425, doi:10.1038/17103.

Wade, J. A., et al. (2005), The May 2003 eruption of Anatahan volcano, Mariana Islands: Geochemical evolution of a silicic island-arc volcano, *J. Volcanol. Geotherm. Res.*, *146*, 139–170, doi:10.1016/j.jvolgeores.2004.11.035.

Wallace, P. J. (2005), Volatiles in subduction zone magmas: Concentrations and fluxes based on melt inclusion and volcanic gas data, *J. Volcanol. Geotherm. Res.*, *140*, 217–240, doi:10.1016/j.jvolgeores.2004.07.023.

Wentz, F. J., C. Gentemann, D. Smith, and D. Chelton (2000), Satellite measurements of sea surface temperature through clouds, *Science*, *288*, 847–850, doi:10.1126/science.288.5467.847.

Wilson, C., and V. J. Coles (2005), Global climatological relationships between satellite biological and physical observations and upper ocean properties, *J. Geophys. Res.*, *110*, C10001, doi:10.1029/2004JC002724.

Wong, G. T. F., S.-W. Chung, F.-K. Shiah, C.-C. Chen, L.-S. Wen, and K.-K. Liu (2002), Nitrate anomaly in the upper nutricline in the northern South China Sea—Evidence for nitrogen fixation, *Geophys. Res. Lett.*, *29*(23), 2097, doi:10.1029/2002GL015796.

Wu, J., W. Sunda, E. A. Boyle, and D. M. Karl (2000), Phosphate depletion in the western North Atlantic Ocean, *Science*, *289*, 759–762, doi:10.1126/science.289.5480.759.

Wu, J., E. A. Boyle, W. Sunda, and L. S. Wen (2001), Soluble and colloidal iron in oligotrophic North Atlantic and North Pacific oceans, *Science*, *293*, 847–849, doi:10.1126/science.1059251.

J.-P. Chen, C.-W. Huang, and I.-I. Lin, Department of Atmospheric Sciences, National Taiwan University, 1, Section 4, Roosevelt Road, Taipei 106, Taiwan. (iilin@as.ntu.edu.tw)

D. A. Chu, Goddard Earth Sciences and Technology Center, NASA Goddard Space Flight Center, Greenbelt, MD 20771, USA.

T. P. Fischer, Department of Earth and Planetary Sciences, University of New Mexico, Albuquerque, NM 87131, USA.

T.-Y. Ho and G. T. F. Wong, Research Centre for Environmental Changes, Academia Sinica, Taipei 115, Taiwan.

C. Hu, College of Marine Sciences, University of South Florida, St. Petersburg, FL 33701, USA.

D. S. Ko, Naval Research Laboratory, Stennis Space Center, MS 39529, USA.

Y.-H. Li, Department of Oceanography, School of Ocean and Earth Science and Technology, University of Hawai'i at Mānoa, Honolulu, HI 96822, USA.

J. Wu, Rosenstiel School of Marine and Atmospheric Science, University of Miami, Miami, FL 33149, USA.